Dynamic succession of groundwater sulfate-reducing communities during prolonged reduction of uranium in a contaminated aquifer

Ping Zhang, Zhili He, Joy D. Van Nostrand, Yujia Qin, Ye Deng, Liyou Wu, Qichao Tu, Jianjun Wang, Christopher W. Schadt, Matthew W. Fields, Terry C. Hazen, Adam P. Arkin, David A. Stahl, and Jizhong Zhou

Supporting Information

A. **Supporting Materials and Methods (6 pages)**

B. **Supporting 11 Figures**

C. **Supporting 2 Tables**

D. **Supporting References**

A. Supporting Materials and Methods

Site description. This study was performed in Area 2 of the US Department of Energy's Oak Ridge Integrated Field Research Challenge (ORIFRC) site, TN. The test plot is located about 300 m from the former S-3 waste ponds (the source of contamination). Contaminants in the groundwater (pH 6.6-6.9) were transported through the primary contaminant path and are primarily U (3.8-7.1 µM), sulfate (1.0-1.2 mM) and nitrate (0.2-1.5 mM) with up to $\geq$300 mg/kg U in soil-saprolite.[1] Dissolved oxygen was near zero although oxygen can infiltrate into the upper vadose zone from the atmosphere. The groundwater flows from an upgradient zone across a control well (W8), three injection wells, and then passes through the downgradient zone installed with seven monitoring wells (W1-W7) (Figure 1). With a high hydraulic conductivity (1.3-3.8 $\times$ 10^{-2} cm/sec) and a mean hydraulic gradient of 0.03, the groundwater took 10 hours to flow through the test plot. The groundwater flow pattern was characterized by injecting a potassium bromide solution (450 mg/L, 3,400 L) into the three injection wells over a 1.5h period two months prior to the test. Peak bromide concentrations were then mapped as an indicator of hydraulic connection among the wells (Figure 1).[2] The contaminated zone is an unlined aquifer ~8.0 m below ground (blg). The water table, which varies with rain fall events, is ~4 m blg. Overlying the bedrock are (a) an intact weathered shale saprolite, 6−8 m blg, that has unconsolidated characteristics that retain much of the bedding and fracture structure of the parent rock, and (b) a zone of fill with a mixture of disturbed saprolite and gravel, 0−6.0 m blg.

EVO amendment and sampling. EVO was injected into the unconsolidated zone (gravelly fill above the intact saprolite). The composition of EVO (SRS^{TM}, Terra Systems, Wilmington, DE) was 60% (w/w) vegetable oil, 0.3% yeast extract, 0.05% $(NH_4)_3PO_4$, 6% food grade surfactants (mainly arachidic acid), and reminder was water. An EVO emulsion (680 L SRS^{TM}

diluted to 3,400 L with site groundwater) was evenly injected into three injection wells over a 2-h time period on February 9, 2009. EVO was injected into the unconsolidated zone (gravel fill above the intact saprolite; beneath the water table) using pumps. After injection, groundwater samples were collected from W1-W8 before injection and 4, 17, 31, 80, 140, and 269 days after the injection by pumping. Before sampling, the wells were purged by pumping ~ 3 times the well volume of groundwater into the well to wash out accumulated dead water in the wells. For microbial community analysis, groundwater was filtered on site with sterile 8-µm filters to remove large particles, followed by filtering with 0.2-µm filters to collect biomass. The filters were immediately frozen, shipped on dry ice to the laboratory, and stored at -80 ºC until DNA extraction.

Groundwater geochemical analysis. Groundwater samples for metal analysis (10 mL) were filtered via 0.3 µm filters, acidified with 0.05 ml of concentrated nitric acid, and then stored at 4ºC until analysis. Details for all analytic methods are described previously.[3, 4] Anions (acetate, NO_3^-, Cl^-, and SO_4^{-2}) were analyzed with an ion chromatograph equipped with an IonPac AS-14 analytical column and an AG-14 guard column (Dionex DX-120, Sunnyvale, CA). Cations (e.g., Ag, Ca, Mg, K) were determined using an inductively coupled plasma mass spectrometer (ICPMS) (Perkin Elmer ELAN 6100). Aqueous Fe(II) and total Fe were measured colorimetrically using a HACH DR 2000 spectrophotometer (Hach Chemical, Loveland, CO).[5]

DNA extraction, PCR amplification, and pyrosequencing of dsrA gene fragments. Because the widely used primer set for amplification of *dsrAB* genes generates a fragment size of 1.2-1.7 kb,[6] primers (DSR1F 5'-ACSCACTGGAAGCACG-3' and DSR2R 5'-GATGTCRTCYYKCCAG-3') were designed to obtain *dsrA* gene fragments of ~500 bp suitable for pyrosequencing. DSR1F was from reference[7] and DSR2R was reversed from DSR2F and

modified. The reverse primer was modified so that it provides the highest alignment with *dsrA* sequences from the GenBank database. Both forward and reverse primers were added with unique 8-mer barcodes that were distinct from each other by at least two nucleotides. Tagging both primers allowed separate use of either forward or reverse sequences, and combined for longer and greater numbers of sequences as well as improved sequence accuracy and reliability.

The community DNA was extracted using a freeze-grinding method[8] and quantified with PicoGreen (Quant-It PicoGreen kit; Invitrogen, Carlsbad, CA). DNA template (50 ng) was combined with a PCR mixture contained 2 U AccuPrime high-fidelity Taq DNA polymerase (Invitrogen, Carsbad, CA), 10 µl buffer containing 2 mM each deoxynucleoside triphosphate, 0.1 µM each primer, 2 mM $MgCl_2$, 0.1 µg/µl bovine serum albumin (New England Biolabs, Beverly, MA), and brought to 100 µl. DNA samples were amplified in triplicate using the following PCR conditions: 94°C for 2 min; 94°C for 30 s, 54°C for 1 min, and 72°C for 1 min for 30 cycles; and 72°C for 7 min. PCR products were pooled and purified by agarose gel electrophoresis and bands of ~600 bp were excised. Bands were extracted with a QIAquick gel extraction kit (Qiagen Inc., Valencia, CA) and cleaned for a second time with the QIAquick PCR purification kit (Qiagen Inc.). Clean products were quantified with PicoGreen and mixed in equal amounts (23 ng each) for 454 pyrosequencing with a Genome Sequencer FLX system (Life Sciences). Due to limited biomass in the groundwater without EVO stimulation and when EVO decreased, limited DNAs were obtained from some samples. These included samples collected from W1-W7 before EVO amendment (W2, W3, W4, W6 and W7), at later stage (day 269) after the amendment (W4, W6 and W7), and from W8 (at days 0, 140 and 269). Therefore, only 44 samples were successfully amplified and sequenced for *dsrA* genes.

PCR amplification and MiSeq sequencing of 16S rRNA genes. The primers 515F (5′ - GTG CCAG CMGC CGCG GTAA-3′) and 806R (5′-GGAC TACH VGGG TWTC TAAT-3′) were used to amplify the V4 region of the 16S rRNA gene.[9] PCR was conducted in a 25 μL mixture containing 0.1 μL of AccuPrime High Fidelity Taq Polymerase (Invitrogen, USA), 2.5 μL of 10× AccuPrime PCR buffer II, 1 μL of each primer (10 μM), 1 μL of template DNA and 19.4 μL of nuclease-free water under the following conditions: 94 °C for 1 min; 35 cycles of 94 °C for 20 s, 53 °C for 25 s, and 68 °C for 45 s; final extension at 68 °C for 10 min. Each sample was amplified in triplicate. PCR products were pooled, purified through QIAquick Gel Extraction Kit (Qiagen), and quantified by Pico Green analysis. The 16S rRNA high-throughput sequencing was conducted on Illumina MiSeq platform at the Institute for Environmental Genomics, University of Oklahoma.

Sequence processing and statistical data analyses. A total of 435,725 raw sequences were obtained and sorted based on barcodes and primers. The quality trimming tool LUCY was used to trim and remove low quality sequences based on their quality scores.[10] Sequences with lengths less than 200 bp or containing any N's were also removed to ensure the quality of remaining sequences. Frame shifts caused by sequencing insertion and deletion errors were checked using FrameBot (http://fungene.cme.msu.edu/FunGenePipeline/resources/fbhelp.jsp) and corrected by comparing the obtained sequences to known reference protein sequences. Forward and reverse sequences were assembled if they had an overlap longer than 20 bp with no more than 2 mismatches. After assembling, 254,801 sequences remained for OTU identification. Clustering tools (UClust, CD-HIT) in Qiime were used when generating OTUs at a 94% similarity level.[11-13] The average nucleotide identity was used for microbial species definition in the postgenomic era.[14, 15] Chimeric sequences were then removed by Chimera Slayer in Qiime.[16] To further

reduce potential pyrosequencing errors, singleton reads for all 44 samples were also eliminated.[17] Finally, a random resampling effort of 2000 sequence per sample was performed and data were used for further statistical analysis.

Various statistical approaches were used to analyze the data as described elsewhere.[18] Hierarchical clustering of all OTUs and samples was used to evaluate differences in SRB community composition and structure. An indicator species approach was used on the resulting clustering topology to find *dsrA* sequences that represent specific sample clusters.[19] This method was chosen because it easily deals with high numbers of sequences per sample. It has been used to identify indicator sequences characterizing different bioactivity conditions and the result provides statistical support for the conclusions.[20] An indicator value (range, 0 to 1) was generated for each OTU-sample cluster combination using both frequency of occurrence and relative abundance information.[19] The indicator value of OTU i in cluster j (e.g., 4-31d) was calculated as follows:

$$\text{Indicator value } I_{ij} = A_{ij}B_{ij}, \text{ and } A_{ij} = \frac{m_{ij}}{\sum_{u=1}^{n} m_{iu}}$$

where A_{ij} is a measure of specificity of OTU i in cluster j, m_{ij} is the average relative abundance of OTU i cross cluster j samples and is calculated as the total relative abundance of OTU i detected in cluster j samples divided by the number of samples in cluster j. B_{ij} is the frequency of occurrence of OTU i in cluster j samples and is calculated as the total number of samples in cluster j that were detected with OTU i divided by the number of samples in cluster j. n is the total cluster number and is 4 in this study.

Other statistical approaches used included (i) microbial diversity indices and significance tests by the Student's t test; (ii) detrended correspondence analysis (DCA) to evaluate differences in key groundwater variables; (iii) analysis of similarity (ANOSIM), permutational multivariate

analysis of variance (Adonis), and multiresponse permutation procedure (MRPP) analysis to determine differences in SRB communities; and (iv) canonical correspondence analysis to link SRB community structure with groundwater variables.
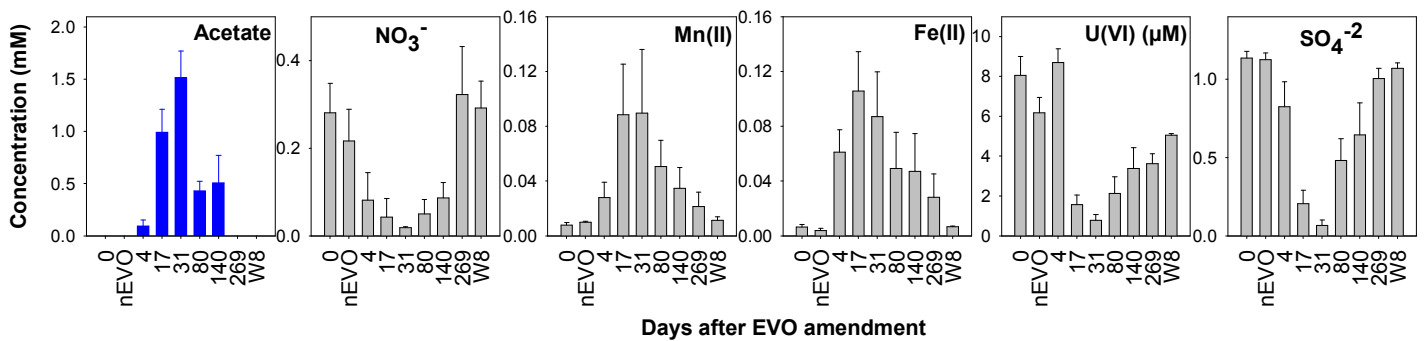
B. Supporting 11 Figures

Figure S1. Changes of average groundwater concentrations of acetate (blue), soluble electron acceptors (NO_3^-, U(VI), and SO_4^{-2}) and reduced products (Fe(II) and Mn(II)) (grey) in the seven downgradient wells (W1 to W7) after EVO amendment as compared to before amendment (0d). Data detected at the same time points in a upgradient control well (W8) and in the non-EVO samples (nEVO) were also included for comparison. Due to limited DNA amounts, we did not obtain *dsrA* PCR products from some samples. The nEVO samples included two samples (W1 and W5) collected at 0d and four samples collected from W8 at days 4, 17, 31, and 80. The day 269 data are from four wells only (W1, W2, W3 and W5). All data are presented as mean ± standard error (SE) of measurements. Detailed changes of these variables in each well are shown in Figure S2 in the supporting information.
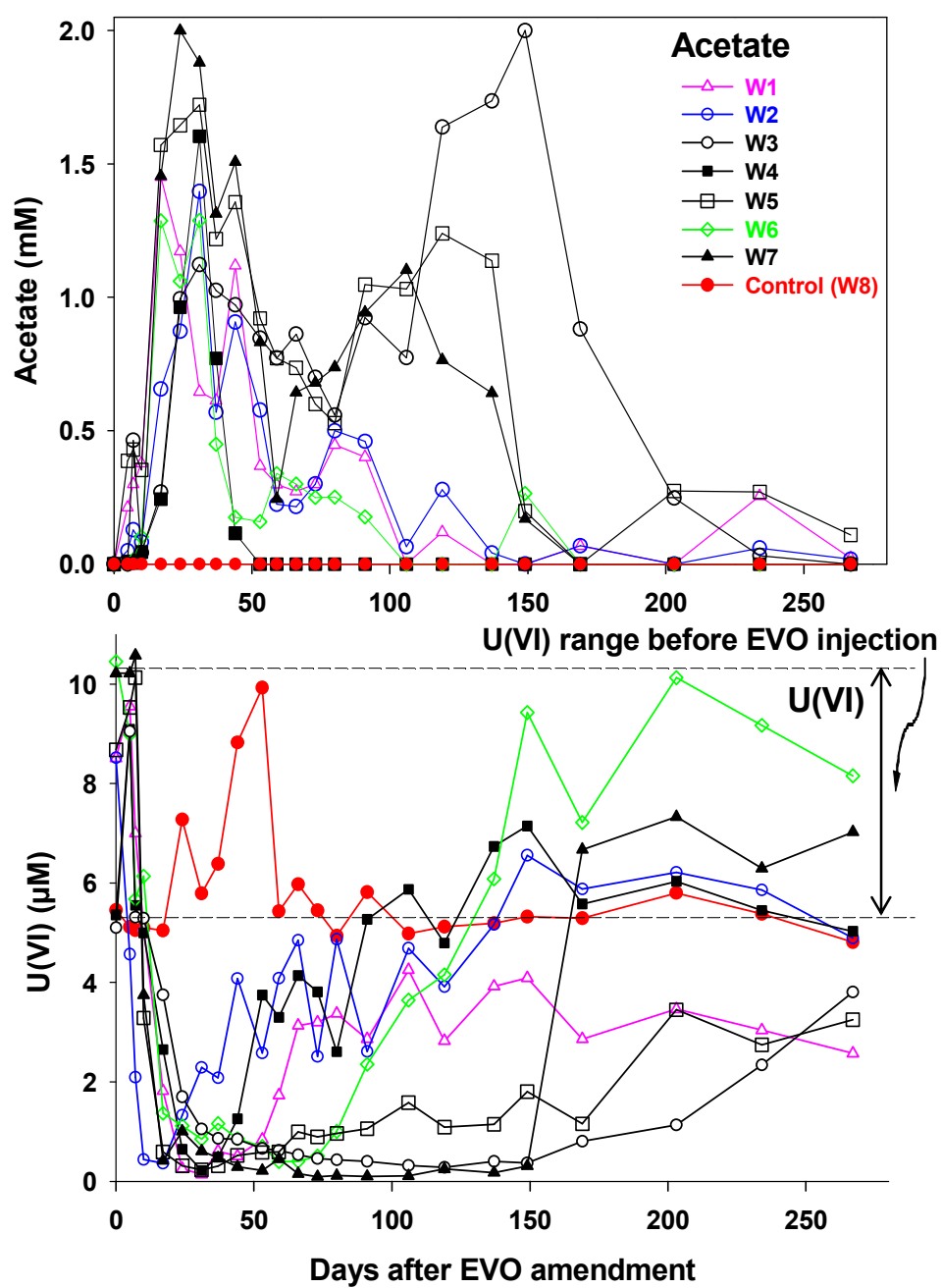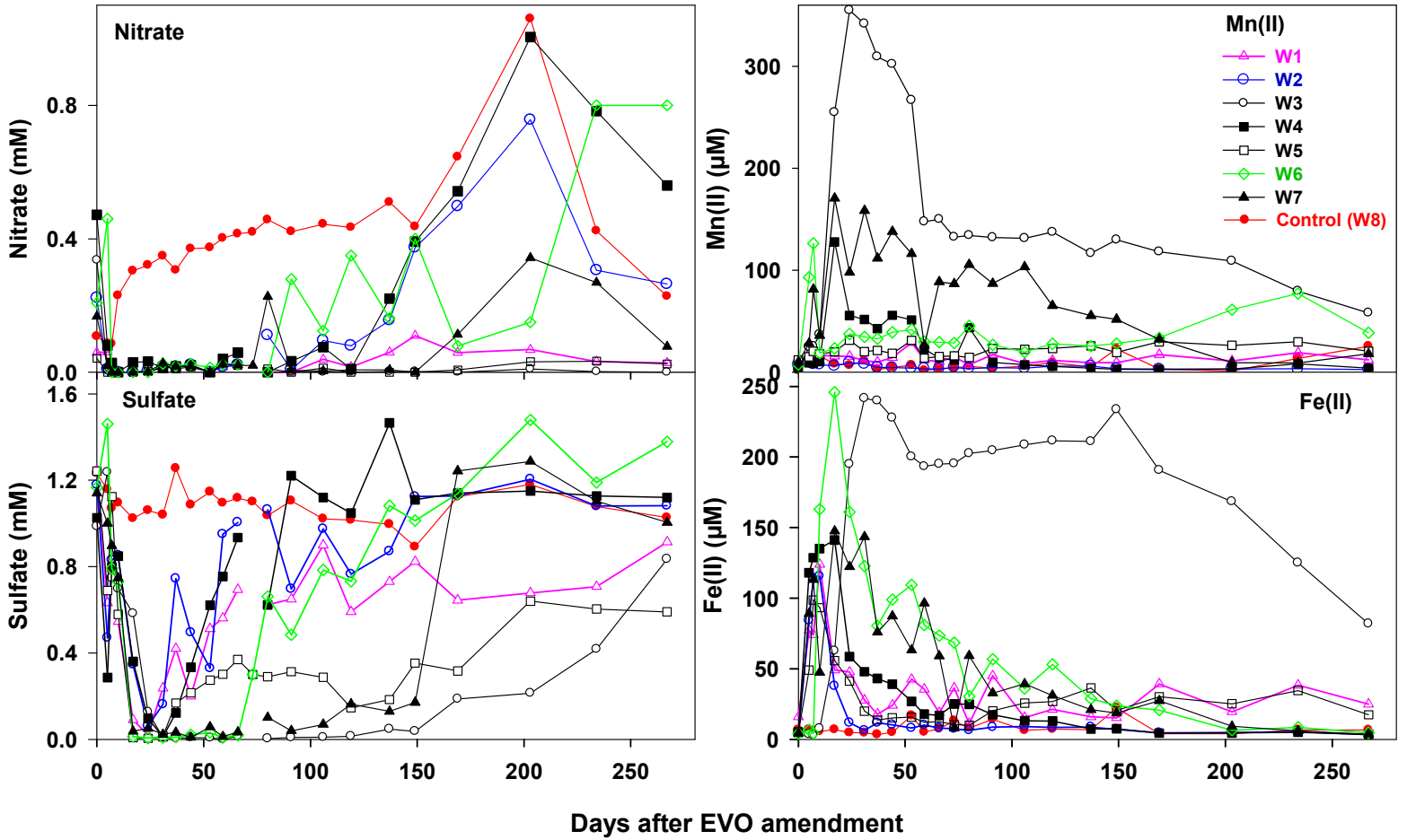
Figure S2. Changes in groundwater concentrations of acetate, U(VI), nitrate, sulfate, Mn(II), and Fe(II) in the eight monitoring wells (W1 to W8) after EVO amendment. The U(VI) concentration range before EVO injection is shown. These data have been reported previously.[2, 21]
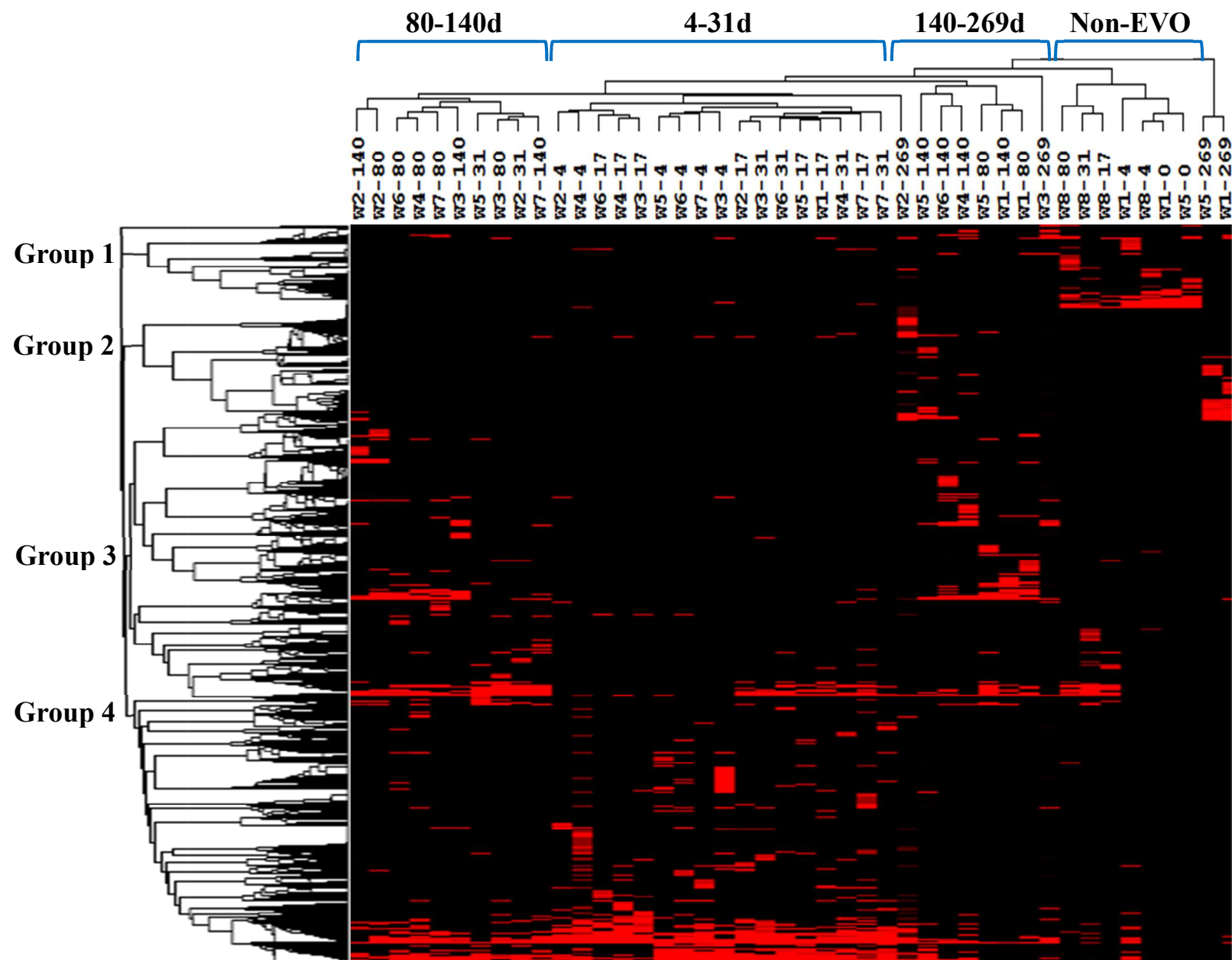
Figure S3. Hierarchical cluster analysis of all OTUs detected. In the sample identification, the number following the dash indicates the sampling day after EVO amendment, with 0 = before amendment. Results were generated in Cluster3.0 and visualized using TreeView. Red indicates presence of the OTU while black indicates absence of the OTU. Brighter red indicates higher gene relative abundance.
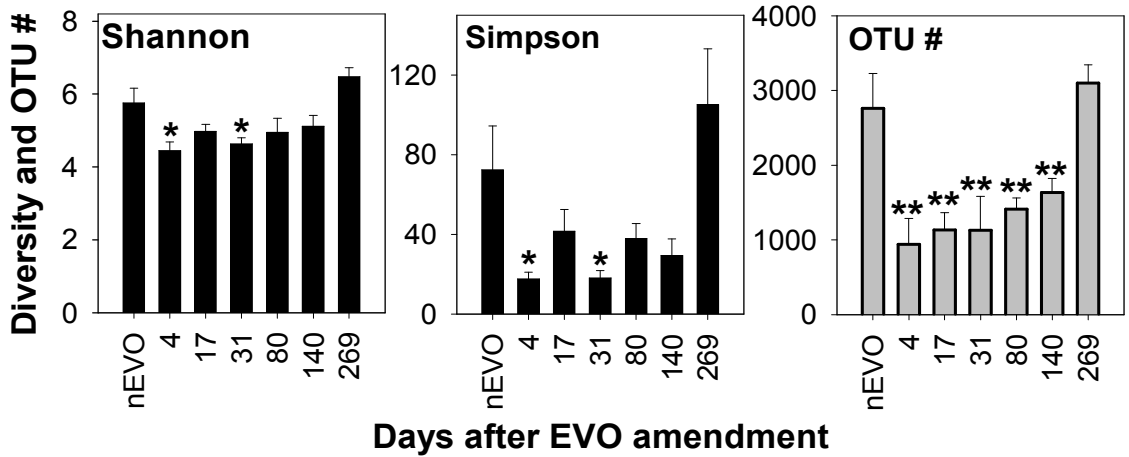
(A) dsrA pyrosequencing
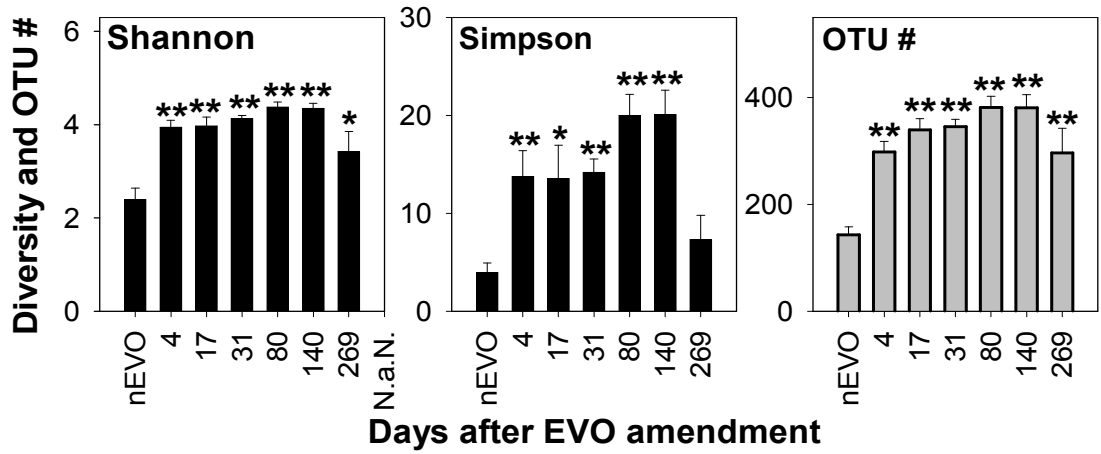
(B) 16S MiSeq all OTUs
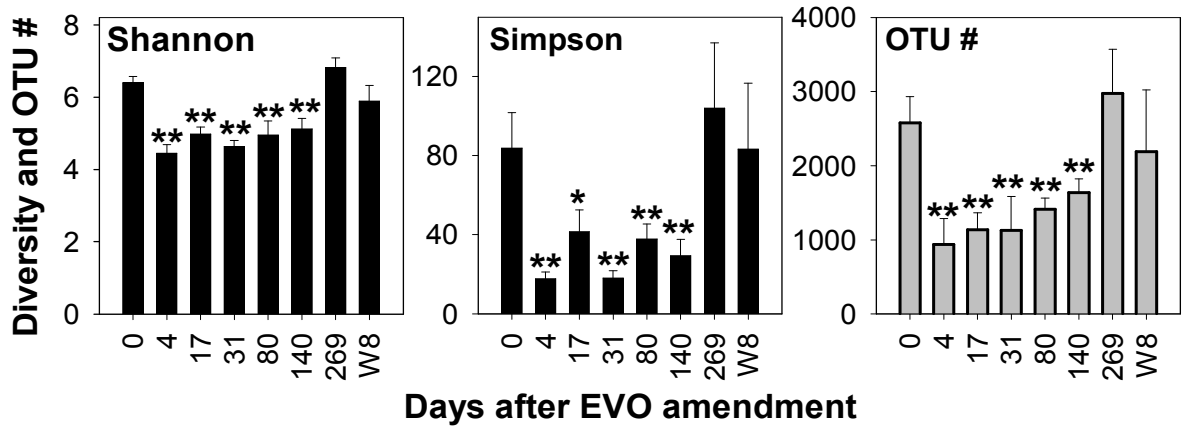
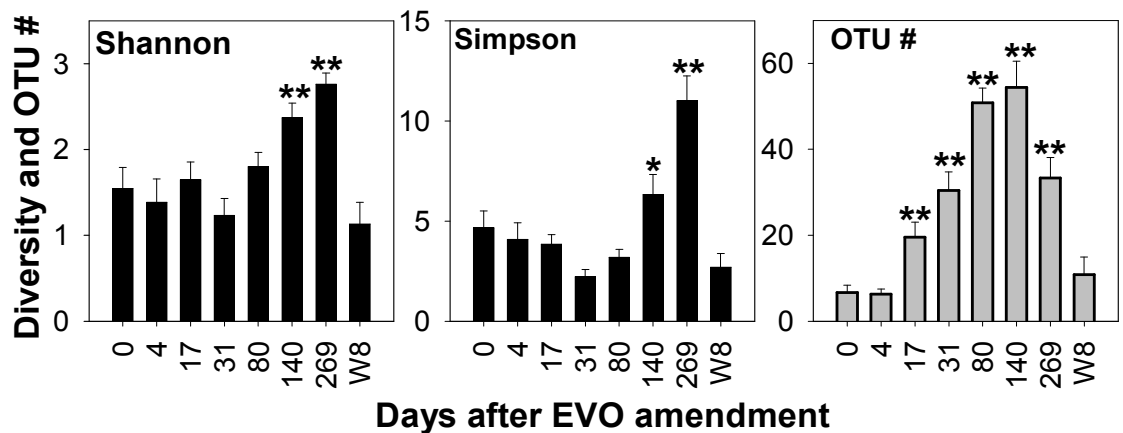**(C) 16S MiSeq all OTUs**

(D) 16S MiSeq 3 SRB families

Figure S4. Enrichment of SRB in the groundwater microbial communities as revealed by *dsrA* gene pyrosequencing and 16S rRNA gene MiSeq sequencing. (A) *dsrA* gene pyrosequencing. Due to limited DNA amounts, we did not obtain *dsrA* PCR products from some samples. The non-EVO (nEVO) samples included two samples (W1 and W5) collected at 0d and four samples collected from W8 at days 4, 17, 31, and 80. The day 269 data are from four wells only (W1, W2, W3 and W5). (B) 16S rRNA gene MiSeq sequencing results of all 56 samples from EVO injection experiment (W1 to W8 at 7 time points). (C) 16S rRNA gene MiSeq sequencing results of 44 samples as those for *dsrA* pyrosequencing. Figures B and C show that the diversity and richness of overall microbial communities decreased after EVO amendment. This was true no matter if we plotted all 56 samples from the experiment or only plotted 44 samples from which we got *dsrA* data. (D) 16S rRNA gene MiSeq sequencing reads classified as *Desulfobacteraceae*, *Desulfovibrionaceae*, and *Desulfobulbaceae*. These three are the dominant families of known SRB detected in this EVO amendment experiment. MiSeq reads were resampled at 10,000 per sample. Data are presented as mean ± standard error (SE) of measurements. For 56 samples, *P* values (**<0.01, *<0.05) from the Student t test are relative to before EVO amendment (0d). For 44 samples, *P* values are relative to non-EVO (nEVO).

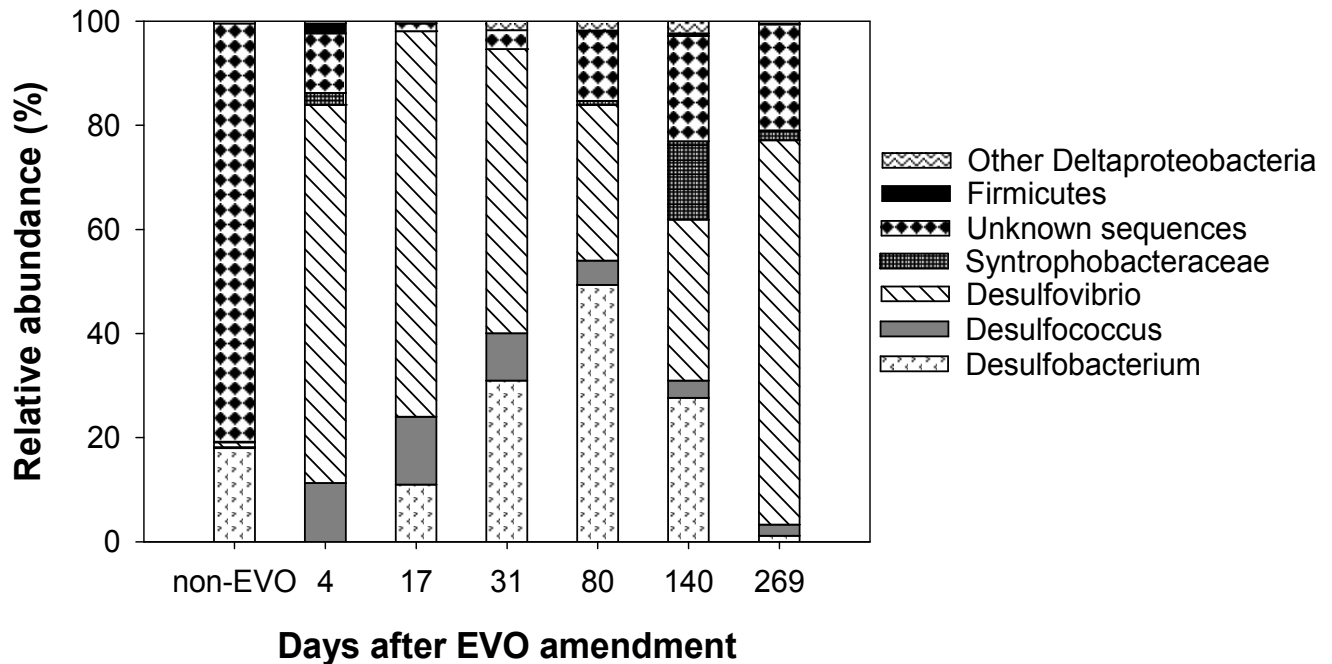**Figure S5.** Changes in SRB community composition after EVO amendment. *Firmicutes* are *Desulfotomaculum* and *Desulfosporosinus*. *Syntrophobacteraceae* included *Desulfacinum*, *Desulfovirga*, *Syntrophobacter*, and unclassified genera in this family. Other *Deltaproteobacteria* are SRB in low abundances, including *Desulfosarcina*, *Desulfarculus*, *Desulfobulbus*, *Desulfocella*, and *Desulfobacter*.

Figure S6. Distribution of top 15 significant indicators of non-EVO cluster in all 44 samples. The closest classifications and indicator values are shown. The highlighted OTUs are included in the phylogenetic analysis (Figure 4). See the supplementary Figure S3 legend for heatmap preparation and explanation.
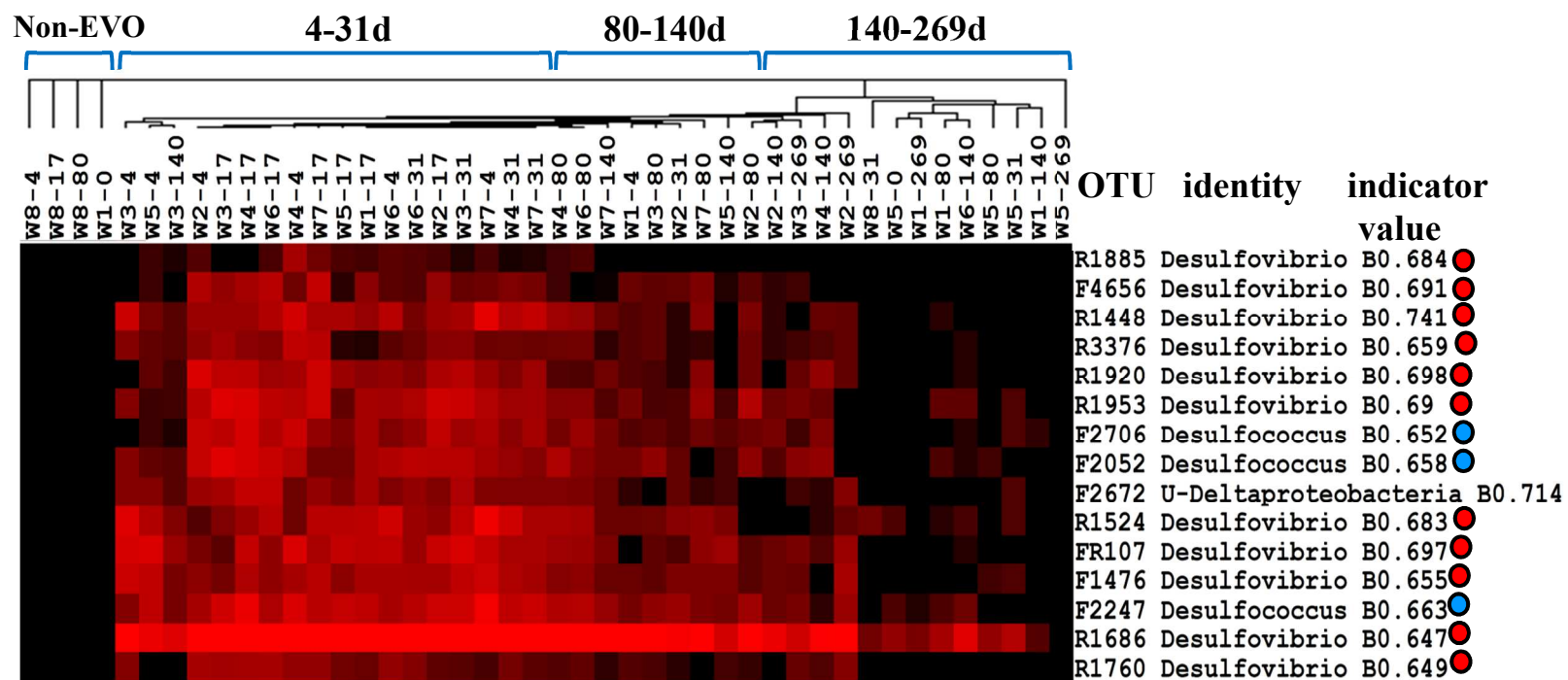
Figure S7. Distribution of top 15 significant indicators of 4-31d in all 44 samples. The closest classifications and indicator values are shown. The highlighted OTUs are included in the phylogenetic analysis (Figure 4). See the supplementary Figure S3 legend for heatmap preparation and explanation.
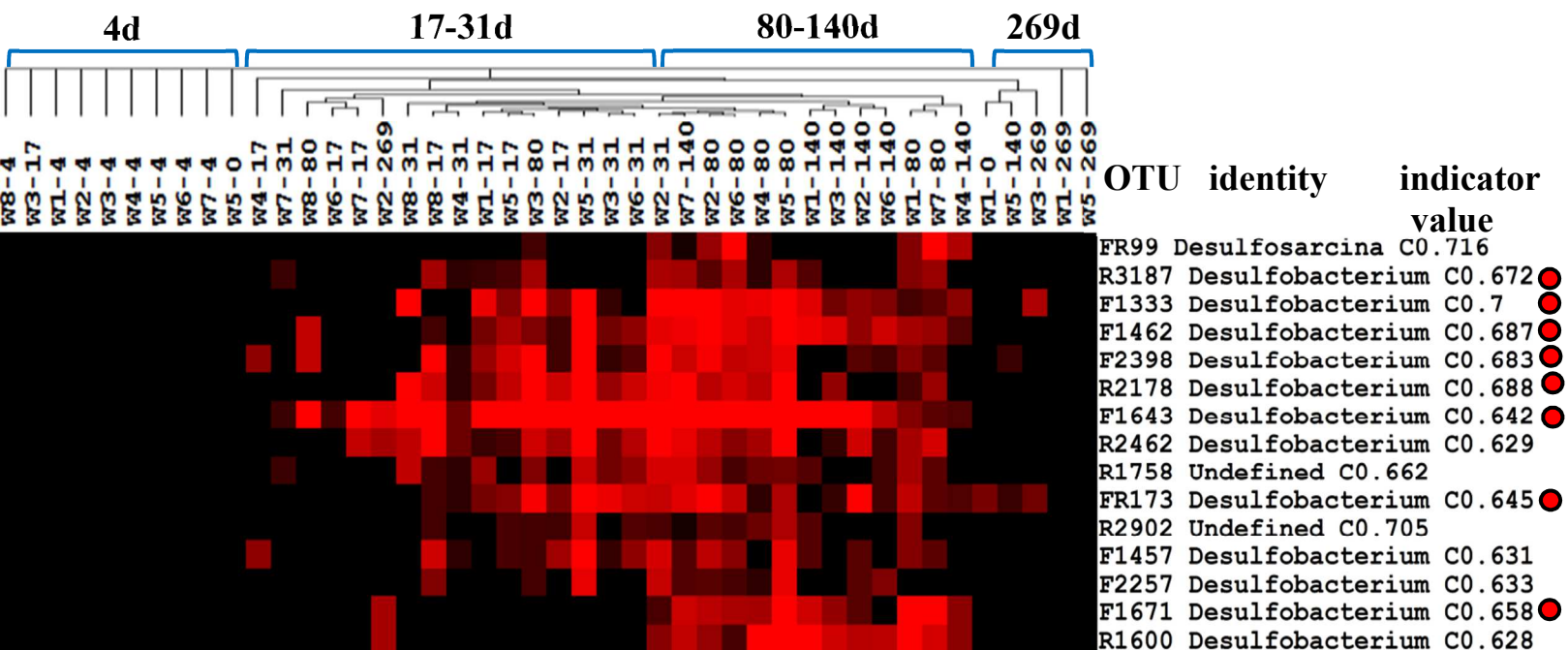
Figure S8. Distribution of top 15 significant indicators of 80-140d in all 44 samples. The closest classifications and indicator values are shown. The highlighted OTUs are included in the phylogenetic analysis (Figure 4). See the supplementary Figure S3 legend for heatmap preparation and explanation.
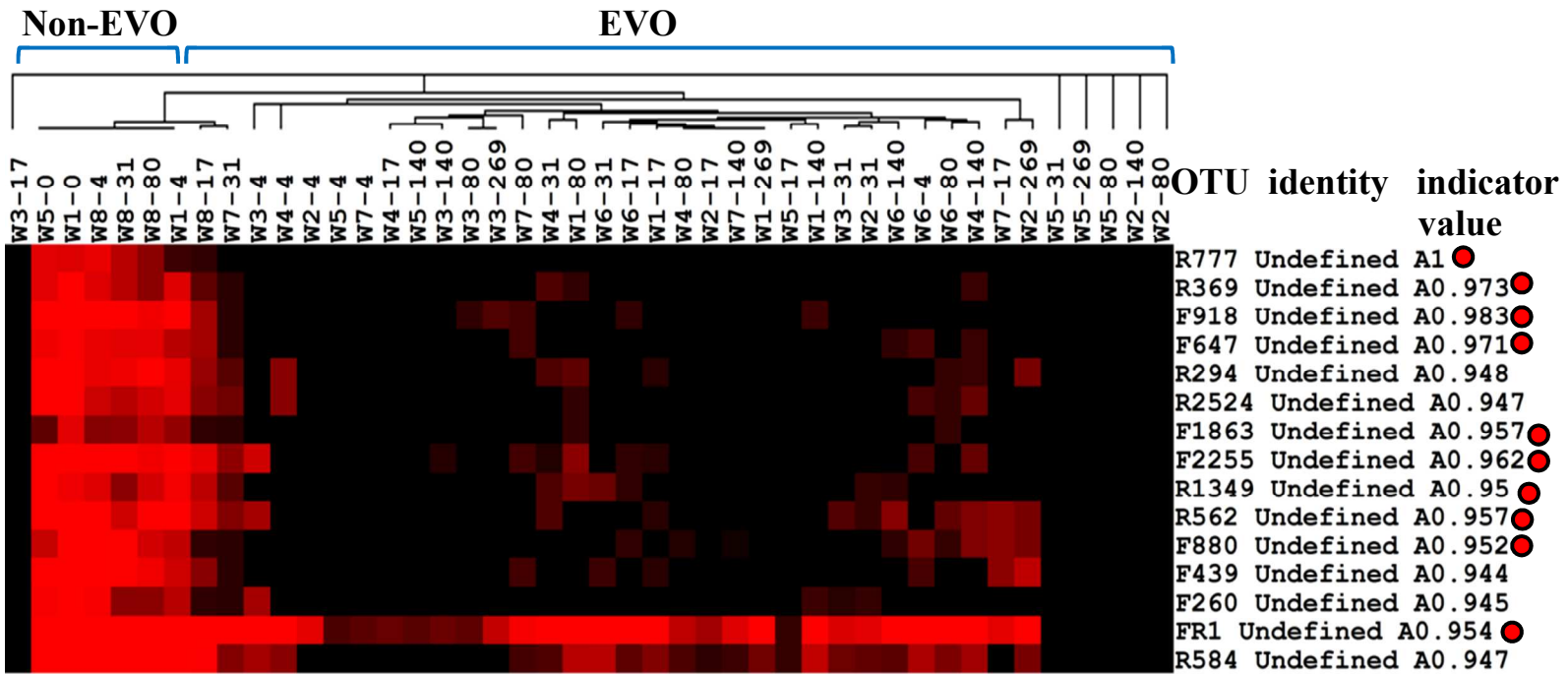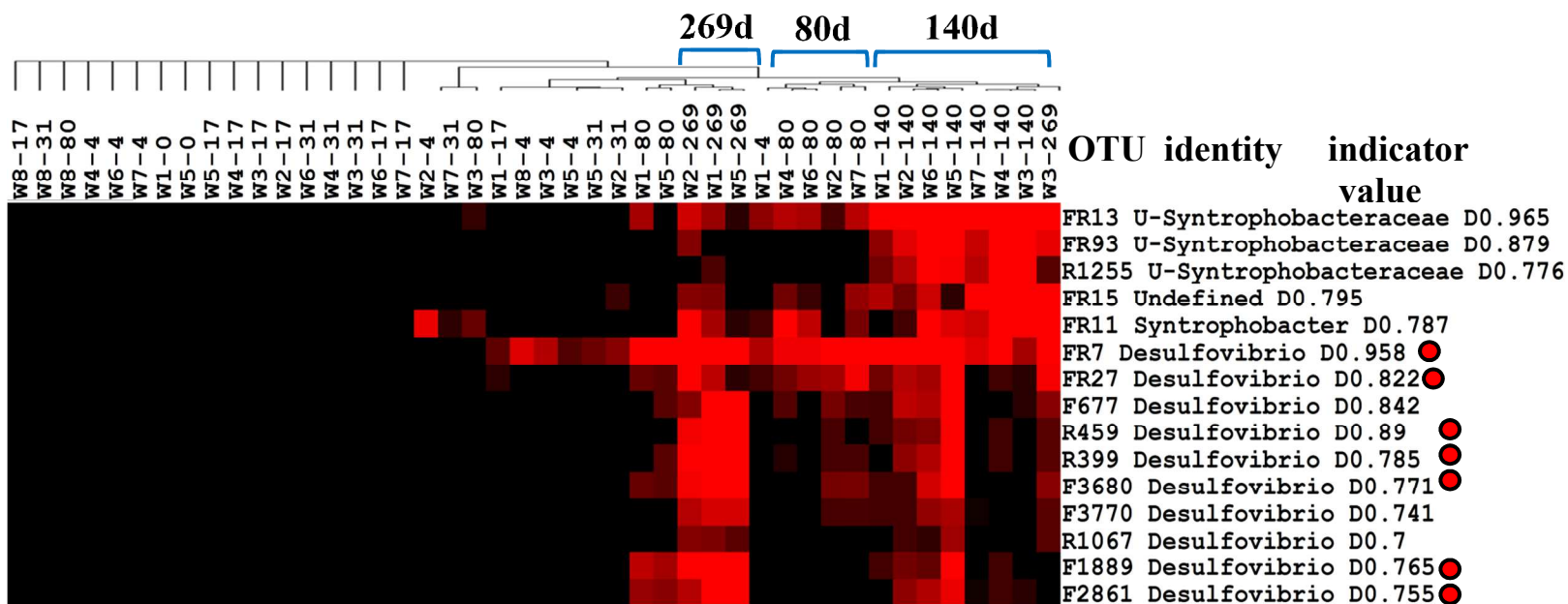

Figure S9. Distribution of top 15 significant indicators of 140-269d in all 44 samples. The closest classifications and indicator values are shown. The highlighted OTUs are included in the phylogenetic analysis (Figure 4). See the supplementary Figure S3 legend for heatmap preparation and explanation.
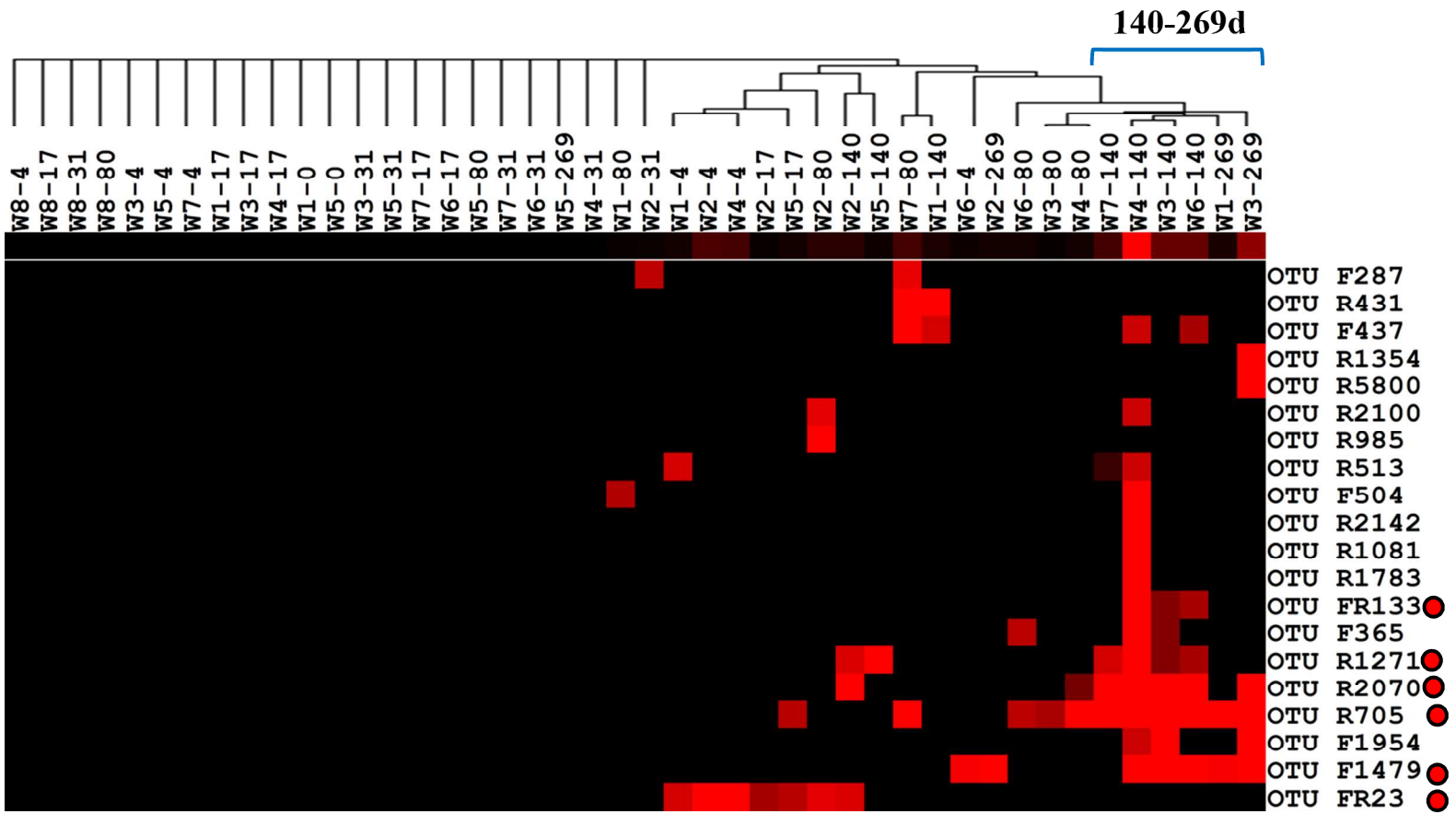
Figure S10. Distribution of detected *Desulfotomaculum*-like OTUs in all 44 samples. The highlighted OTUs are included in the phylogenetic analysis (Figure 4). See the supplementary Figure S3 legend for heatmap preparation and explanation.
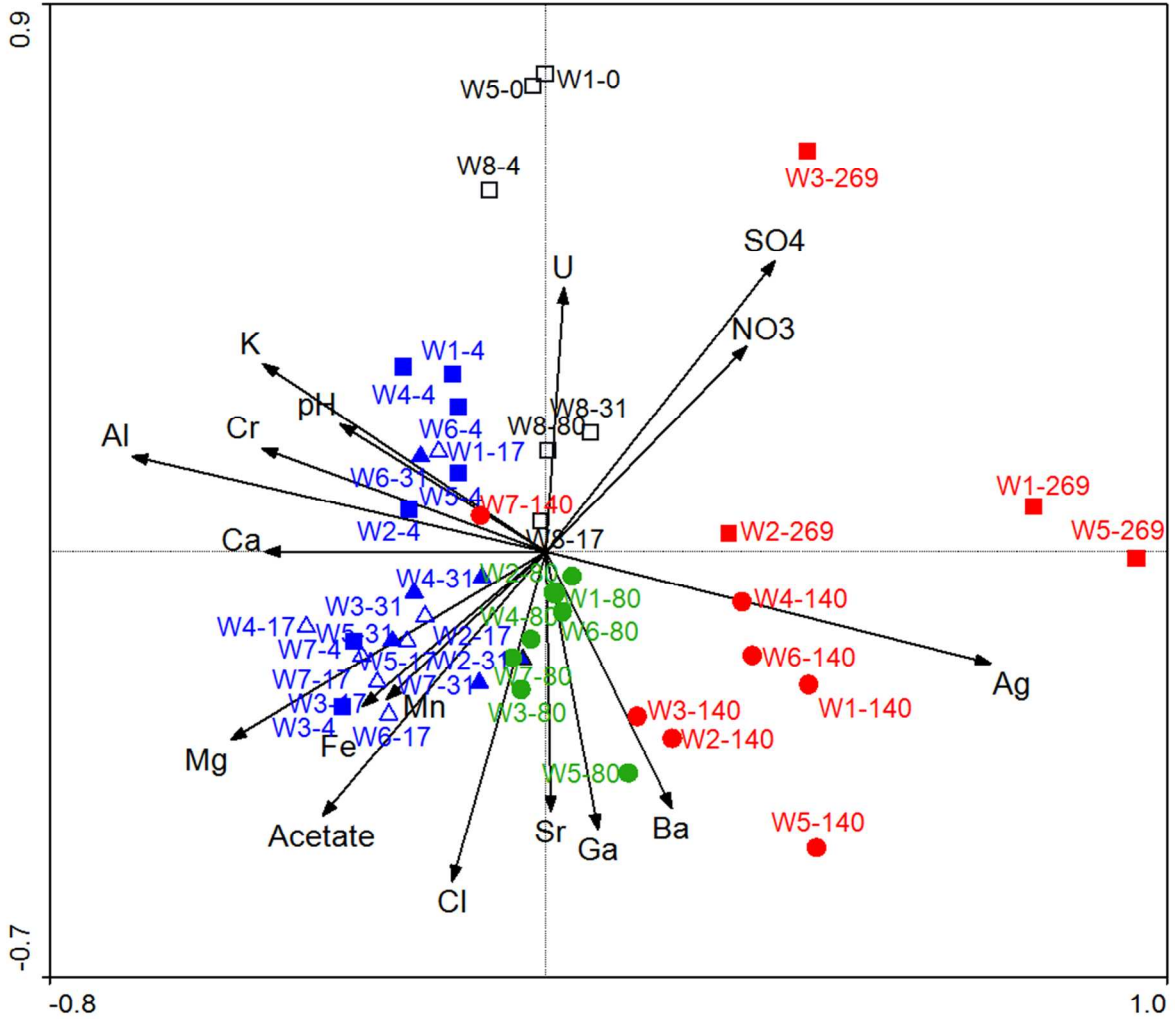
Figure S11. Canonical correspondence analysis (CCA) shows significant ($P = 0.004$) correlations between relative abundance of all detected OTUs (symbols) and environmental variables (arrows). Environmental variables were chosen based on significance calculated from individual CCA results and variance inflation factors (VIFs < 20) calculated during CCA. This model explained 62% of the variations in the SRB community structure. In the sample identification, the number following the dash indicates the sampling day after EVO amendment, with 0 = before amendment.

C. Supporting 2 Tables

Table S1. Changes in the composition and structure of groundwater SRB communities after EVO amendment revealed by three statistical tests[a]

Sample groups	MRPP	ANOSIM	Adonis
Non-EVO **vs**. 4-31d	0.48 (**0.001**)[b]	0.98 (**0.001**)	0.51 (**0.001**)
Non-EVO **vs**. 80-140d	0.52 (**0.001**)	0.82 (**0.001**)	0.46 (**0.001**)
Non-EVO **vs**. 140-269d	0.68 (**0.001**)	0.71 (**0.001**)	0.31 (**0.001**)
4-31d **vs**. 80-140d	0.48 (**0.001**)	0.62 (**0.001**)	0.28 (**0.001**)
4-31d **vs**. 140-269d	0.58 (**0.001**)	0.78 (**0.001**)	0.31 (**0.001**)
80-140d **vs**. 140-269d	0.65 (**0.001**)	0.33 (**0.001**)	0.18 (**0.001**)
4d **vs**. 17d	0.46 (0.136)	0.16 (0.105)	0.14 (0.138)
17d **vs**. 31d	0.42 (0.248)	0.01 (0.343)	0.10 (0.297)
80d **vs**. 140d	0.52 (0.557)	0.17 (0.168)	0.14 (0.403)
140d **vs**. 269d	0.71 (0.082)	0.33 (0.058)	0.26 (0.056)

[a]All three tests are non-parametric multivariate analyses based on dissimilarities between samples in different groups using bray-cutis distance. MRPP, multiple response permutation procedure, a nonparametric procedure that does not depend on assumptions such as normally distributed data or homogeneous variances, but rather depends on the internal variability of the data; ANOSIM, analysis of similarity; Adonis, non-parametric multivariate analysis of variance (MANOVA) with the adonis function.

[b]Statistic (P value). The difference is significant when at least two tests gave P values of < 0.05 (bold).

Table S2. Top 30 significant indicators identified by clustering and indicator species analyses of all detected OTUs (SI Figure S3). These indicator SRB characterized the different bioactivity stages defined based on groundwater concentrations of acetate, NO_3^-, Mn(II), Fe(II), U(VI), and SO_4^{-2} (Figure 2)

Non-EVO	species	value[a]	4-31d	species[c]	value	80-140d	species	value	140-269d	species	value
OTU-R777	N[b]	1.00	OTU-R1448	Desulfovibrio	0.74	OTU-FR99	Desulfosarcina	0.72	OTU-FR13	Syntrophobacteraceae	0.97
OTU-F918	N	0.98	OTU-F2672	δ-Proteobacteria	0.71	OTU-R2902	N	0.70	OTU-FR7	Desulfovibrio	0.96
OTU-R369	N	0.97	OTU-R1920	Desulfovibrio	0.70	OTU-F1333	Desulfobacterium	0.70	OTU-R459	Desulfovibrio	0.89
OTU-F647	N	0.97	OTU-FR107	Desulfovibrio	0.70	OTU-R2178	Desulfobacterium	0.69	OTU-FR93	Syntrophobacteraceae	0.88
OTU-F2255	N	0.96	OTU-F4656	Desulfovibrio	0.69	OTU-F1462	Desulfobacterium	0.69	OTU-F677	Desulfovibrio	0.84
OTU-F1863	N	0.96	OTU-R1953	Desulfovibrio	0.69	OTU-F2398	Desulfobacterium	0.68	OTU-FR27	Desulfovibrio	0.82
OTU-R562	N	0.96	OTU-R1885	Desulfovibrio	0.68	OTU-R3187	Desulfobacterium	0.67	OTU-FR15	N	0.79
OTU-FR1	N	0.95	OTU-R1524	Desulfovibrio	0.68	OTU-R1758	N	0.66	OTU-FR11	Syntrophobacter	0.79
OTU-F880	N	0.95	OTU-F2247	Desulfococcus	0.66	OTU-F1671	Desulfobacterium	0.66	OTU-R399	Desulfovibrio	0.78
OTU-R1349	N	0.95	OTU-R3376	Desulfovibrio	0.66	OTU-FR173	Desulfobacterium	0.65	OTU-R1255	Syntrophobacteraceae	0.78
OTU-R294	N	0.95	OTU-F2052	Desulfococcus	0.66	OTU-F1643	Desulfobacterium	0.64	OTU-F3680	Desulfovibrio	0.77
OTU-R2524	N	0.95	OTU-F1476	Desulfovibrio	0.65	OTU-F2257	Desulfobacterium	0.63	OTU-F1889	Desulfovibrio	0.76
OTU-R584	N	0.95	OTU-F2706	Desulfococcus	0.65	OTU-F1457	Desulfobacterium	0.63	OTU-F2861	Desulfovibrio	0.75
OTU-F260	N	0.95	OTU-R1760	Desulfovibrio	0.65	OTU-R2462	Desulfobacterium	0.63	OTU-F3770	Desulfovibrio	0.74
OTU-F439	N	0.94	OTU-R1686	Desulfovibrio	0.65	OTU-R1600	Desulfobacterium	0.63	OTU-R1067	Desulfovibrio	0.70
OTU-R2677	N	0.94	OTU-R1200	Desulfovibrio	0.65	OTU-F380	Desulfobacterium	0.62	OTU-F449	Desulfovibrio	0.70
OTU-R2037	N	0.93	OTU-R1792	Desulfovibrio	0.65	OTU-F1376	Desulfobacterium	0.62	OTU-R2024	Syntrophobacteraceae	0.69
OTU-F650	N	0.93	OTU-F1493	Desulfococcus	0.64	OTU-F1758	Desulfobacterium	0.61	OTU-F689	Desulfovibrio	0.69
OTU-R879	N	0.87	OTU-R2096	Desulfovibrio	0.64	OTU-F1288	Desulfobacterium	0.60	OTU-R536	Desulfovibrio	0.69
OTU-F899	N	0.86	OTU-R3274	Desulfovibrio	0.64	OTU-F1461	Desulfocella	0.60	OTU-R275	Desulfovibrio	0.69
OTU-R3375	N	0.84	OTU-R2546	Desulfovibrio	0.64	OTU-R2326	N	0.60	OTU-R356	Desulfovibrio	0.69
OTU-F770	N	0.84	OTU-R2274	Desulfovibrio	0.64	OTU-F1890	Desulfobacterium	0.60	OTU-R1199	Syntrophobacteraceae	0.69
OTU-F905	N	0.84	OTU-F2024	Desulfococcus	0.64	OTU-F1767	Desulfobacterium	0.60	OTU-F1896	Syntrophobacter	0.68
OTU-F2149	N	0.84	OTU-F1141	Desulfococcus	0.64	OTU-R1977	Desulfobacterium	0.60	OTU-R279	Desulfovibrio	0.68
OTU-F3813	N	0.84	OTU-R1833	Desulfovibrio	0.64	OTU-R2506	Desulfobacterium	0.60	OTU-F860	Desulfovibrio	0.68
OTU-R425	N	0.84	OTU-F1260	Desulfococcus	0.63	OTU-F1426	Desulfobacterium	0.59	OTU-FR41	δ-Proteobacteria	0.68
OTU-F386	N	0.83	OTU-R1428	Desulfovibrio	0.63	OTU-R3150	Desulfobacterium	0.59	OTU-R3118	Syntrophobacteraceae	0.67
OTU-F906	N	0.83	OTU-R1315	Desulfovibrio	0.63	OTU-F1190	Desulfobacterium	0.59	OTU-R1539	Syntrophobacteraceae	0.67
OTU-F719	N	0.83	OTU-R2181	Desulfovibrio	0.63	OTU-R1929	N	0.58	OTU-F263	Desulfovibrio	0.67
OTU-F323	N	0.83	OTU-R930	Desulfovibrio	0.63	OTU-F4333	Desulfocella	0.58	OTU-FR39	δ-Proteobacteria	0.66

[a]indicator values, [b]novel at all taxonomy levels, [c]identified lowest taxonomy level

D. Supporting References

(1) Moon, J. W.; Roh, Y.; Phelps, T. J.; Phillips, D. H.; Watson, D. B.; Kim, Y. J.; Brooks, S. C. Physicochemical and mineralogical characterization of soil-saprolite cores from a field research site, Tennessee. *J Environ Qual* **2006,** *35* (5), 1731-1741.

(2) Gihring, T. M.; Zhang, G. X.; Brandt, C. C.; Brooks, S. C.; Campbell, J. H.; Carroll, S.; Criddle, C. S.; Green, S. J.; Jardine, P.; Kostka, J. E.; Lowe, K.; Mehlhorn, T. L.; Overholt, W.; Watson, D. B.; Yang, Z. M.; Wu, W. M.; Schadt, C. W. A Limited Microbial Consortium Is Responsible for Extended Bioreduction of Uranium in a Contaminated Aquifer. *Appl Environ Microb* **2011,** *77* (17), 5955-5965.

(3) Wu, W. M.; Carley, J.; Green, S. J.; Luo, J.; Kelly, S. D.; Van Nostrand, J.; Lowe, K.; Mehlhorn, T.; Carroll, S.; Boonchayanant, B.; Lofller, F. E.; Watson, D.; Kemner, K. M.; Zhou, J. Z.; Kitanidis, P. K.; Kostka, J. E.; Jardine, P. M.; Criddle, C. S. Effects of Nitrate on the Stability of Uranium in a Bioreduced Region of the Subsurface. *Environ Sci Technol* **2010,** *44* (13), 5104-5111.

(4) Wu, W. M.; Carley, J.; Luo, J.; Ginder-Vogel, M. A.; Cardenas, E.; Leigh, M. B.; Hwang, C. C.; Kelly, S. D.; Ruan, C. M.; Wu, L. Y.; Van Nostrand, J.; Gentry, T.; Lowe, K.; Mehlhorn, T.; Carroll, S.; Luo, W. S.; Fields, M. W.; Gu, B. H.; Watson, D.; Kemner, K. M.; Marsh, T.; Tiedje, J.; Zhou, J. Z.; Fendorf, S.; Kitanidis, P. K.; Jardine, P. M.; Criddle, C. S. In situ bioreduction of uranium (VI) to submicromolar levels and reoxidation by dissolved oxygen. *Environ Sci Technol* **2007,** *41* (16), 5716-5723.

(5) Viollier, E.; Inglett, P. W.; Hunter, K.; Roychoudhury, A. N.; Van Cappellen, P. The ferrozine method revisited: Fe(II)/Fe(III) determination in natural waters. *Appl Geochem* **2000,** *15* (6), 785-790.

(6) Karkhoffschweizer, R. R.; Huber, D. P. W.; Voordouw, G. Conservation of the Genes for Dissimilatory Sulfite Reductase from Desulfovibrio-Vulgaris and Archaeoglobus-Fulgidus Allows Their Detection by Pcr. *Appl Environ Microb* **1995,** *61* (1), 290-296.

(7) Wagner, M.; Roger, A. J.; Flax, J. L.; Brusseau, G. A.; Stahl, D. A. Phylogeny of dissimilatory sulfite reductases supports an early origin of sulfate respiration. *J Bacteriol* **1998,** *180* (11), 2975-2982.

(8) Zhou, J. Z.; Bruns, M. A.; Tiedje, J. M. DNA recovery from soils of diverse composition. *Appl Environ Microb* **1996,** *62*, (2), 316-322.

(9) Caporaso, J. G.; Lauber, C. L.; Walters, W. A.; Berg-Lyons, D.; Lozupone, C. A.; Turnbaugh, P. J.; Fierer, N.; Knight, R. Global patterns of 16S rRNA diversity at a depth of millions of sequences per sample. *P Natl Acad Sci USA* **2011,** *108*, 4516-4522.

(10) Chou, H. H.; Holmes, M. H. DNA sequence quality trimming and vector removal. *Bioinformatics* **2001,** *17* (12), 1093-1104.

(11) Edgar, R. C. Search and clustering orders of magnitude faster than BLAST. *Bioinformatics* **2010,** *26* (19), 2460-2461.

(12) Li, W. Z.; Godzik, A. Cd-hit: a fast program for clustering and comparing large sets of protein or nucleotide sequences. *Bioinformatics* **2006,** *22* (13), 1658-1659.

(13) Caporaso, J. G.; Kuczynski, J.; Stombaugh, J.; Bittinger, K.; Bushman, F. D.; Costello, E. K.; Fierer, N.; Pena, A. G.; Goodrich, J. K.; Gordon, J. I.; Huttley, G. A.; Kelley, S. T.; Knights, D.; Koenig, J. E.; Ley, R. E.; Lozupone, C. A.; McDonald, D.; Muegge, B. D.; Pirrung, M.; Reeder, J.; Sevinsky, J. R.; Tumbaugh, P. J.; Walters, W. A.; Widmann, J.; Yatsunenko, T.;

Zaneveld, J.; Knight, R. QIIME allows analysis of high-throughput community sequencing data. *Nat Methods* **2010,** *7* (5), 335-336.

(14) Konstantinidis, K. T.; Tiedje, J. M. Genomic insights that advance the species definition for prokaryotes. *P Natl Acad Sci USA* **2005,** *102* (7), 2567-2572.

(15) Frank, K. L.; Rogers, D. R.; Olins, H. C.; Vidoudez, C.; Girguis, P. R. Characterizing the distribution and rates of microbial sulfate reduction at Middle Valley hydrothermal vents. *Isme J* **2013,** *7* (7), 1391-1401.

(16) Haas, B. J.; Gevers, D.; Earl, A. M.; Feldgarden, M.; Ward, D. V.; Giannoukos, G.; Ciulla, D.; Tabbaa, D.; Highlander, S. K.; Sodergren, E.; Methe, B.; DeSantis, T. Z.; Petrosino, J. F.; Knight, R.; Birren, B. W.; Consortium, H. M. Chimeric 16S rRNA sequence formation and detection in Sanger and 454-pyrosequenced PCR amplicons. *Genome Res* **2011,** *21* (3), 494-504.

(17) Zhou, J.; Wu, L.; Deng, Y.; Zhi, X.; Jiang, Y. H.; Tu, Q.; Xie, J.; Van Nostrand, J. D.; He, Z.; Yang, Y. Reproducibility and quantitation of amplicon sequencing-based detection. *Isme J* **2011,** *5* (8), 1303-13.

(18) He, Z. L.; Xu, M. Y.; Deng, Y.; Kang, S. H.; Kellogg, L.; Wu, L. Y.; Van Nostrand, J. D.; Hobbie, S. E.; Reich, P. B.; Zhou, J. Z. Metagenomic analysis reveals a marked divergence in the structure of belowground microbial communities at elevated CO_2. *Ecol Lett* **2010,** *13* (5), 564-575.

(19) Dufrene, M.; Legendre, P. Species assemblages and indicator species: The need for a flexible asymmetrical approach. *Ecol Monogr* **1997,** *67* (3), 345-366.

(20) Marsh, T. L.; Cardenas, E.; Wu, W. M.; Leigh, M. B.; Carley, J.; Carroll, S.; Gentry, T.; Luo, J.; Watson, D.; Gu, B. H.; Ginder-Vogel, M.; Kitanidis, P. K.; Jardine, P. M.; Zhou, J. Z.; Criddle, C. S.; Tiedje, J. M. Significant Association between Sulfate-Reducing Bacteria and Uranium-Reducing Microbial Communities as Revealed by a Combined Massively Parallel Sequencing-Indicator Species Approach. *Appl Environ Microb* **2010,** *76* (20), 6778-6786.

(21) Watson, D. B.; Wu, W. M.; Mehlhorn, T.; Tang, G.; Earles, J.; Lowe, K.; Gihring, T. M.; Zhang, G.; Phillips, J.; Boyanov, M. I.; Spalding, B. P.; Schadt, C.; Kemner, K. M.; Criddle, C. S.; Jardine, P. M.; Brooks, S. C. In situ bioremediation of uranium with emulsified vegetable oil as the electron donor. *Environ Sci Technol* **2013,** *47* (12), 6440-8.